



ELSEVIER

Available online at www.sciencedirect.com

SCIENCE @ DIRECT®

Journal of Luminescence 104 (2003) 283–294

JOURNAL OF
LUMINESCENCE

www.elsevier.com/locate/jlumin

The analysis of thermoluminescence glow curves

S. Basun^a, G.F. Imbusch^{b,*}, D.D. Jia^c, W.M. Yen^c

^a*A.F. Ioffe Physico-Technical Institute, St. Petersburg, Russia*

^b*Department of Physics, National University of Ireland, Galway, Ireland*

^c*Department of Physics and Astronomy, the University of Georgia, Athens, USA*

Received 15 August 2002; received in revised form 15 January 2003; accepted 3 March 2003

Abstract

Information about the behavior of traps in a luminescent material is usually derived by fitting the glow curves in the thermoluminescence spectrum of the material to a general formula. From the fit one seeks to obtain values for the depth of the traps, the frequency factors governing the release of electrons from the traps, and some indication of the rates of trapping and retrapping. This study investigates how successful this fitting process is in providing reliable values for the trap parameters. The relevant rate equations are used to numerically generate simulated glow curves for specific values of trap parameters. These glow curves are then analyzed by the usual fitting process, and values for the trap parameters are derived from the fitting process. We comment on the comparison between the derived parameter values and the correct values. From these comparisons we attempt to obtain some useful insights to assist in the interpretation of experimentally observed thermoluminescence spectra.

© 2003 Elsevier Science B.V. All rights reserved.

Keywords: Thermoluminescence; Glow curves; Electron traps

1. Introduction

Thermoluminescence is observed when, in the process of irradiating a material, part of the irradiation energy is used to transfer electrons to traps. This energy, stored in the form of the trapped electrons, is released by raising the temperature of the material, and the released energy is converted to luminescence. This trapping process and the subsequent release of the stored energy finds important application in ionizing radiation dosimetry and in the operation of long-persistence phosphors. Much information about

the trapping process and the release of trapped electrons is obtained from the thermoluminescence (TL) spectrum, in which, after turning off the irradiating source, the thermally stimulated luminescence is monitored under a condition of steadily increasing temperature. The shape and position of the resultant TL glow curves can be analyzed to extract information on the various parameters of the trapping process—trap depth, trapping and retrapping rates, etc.

The physical mechanisms governing the trapping and release of electrons are discussed in detail in the text by McKeever [1]. The rate equations describing these physical processes at a single type of trap can be solved, under various assumptions, and analytical expressions are obtained for the

*Corresponding author. Fax: +353-91-525-700.

E-mail address: g.f.imbusch@nuigalway.ie (G.F. Imbusch).

shape of the resulting glow curve. Experimentally observed glow curves are analyzed by fitting them to the analytical expressions, and the parameters are determined from the fitting process [1–3].

The purpose of the present study is to investigate how well this fitting process works in providing reliable values for the parameters of the traps. The relevant rate equations describing the flow of electrons between traps and the luminescence centers are used, without approximation, to numerically generate simulated TL glow curves for a wide range of trap parameters. These simulated glow curves are then analyzed by the usual method of fitting them to one of the analytical expressions, and the parameter values determined by this fitting procedure are compared with the values used in generating the glow curves. We comment on the comparisons, and endeavor to derive some useful insights to assist in the interpretation and analysis of experimentally measured TL glow curves.

2. Analysis of the thermoluminescence process

We first discuss the thermoluminescence process and develop the relevant rate equations. We briefly review the solutions of these rate equations, and the conditions under which first order, second order, and general order kinetics apply.

Radiation with sufficiently energetic photons causes photoionization of the luminescence centers, raising electrons to the conduction band (CB). Some of these electrons are captured by traps and occupy levels at a depth E below the CB. We are concerned here with the mechanism of the release of electrons from the traps after irradiation and their subsequent recombination with the photo-ionized luminescence centers, resulting in radiative emission. A simple model for a luminescent phosphor with a single trap type is shown in Fig. 1.

N_A and N_B , respectively, are the densities of the luminescence centers (in the prepared ionization state) in levels A and B. N^+ is the density of photo-ionized centers. As an illustrative example, the Eu^{2+} ions are the *luminescent centers* in the phosphor $\text{SrAl}_2\text{O}_4:\text{Eu}^{2+}$, Dy^{3+} ; the Dy^{3+} ions

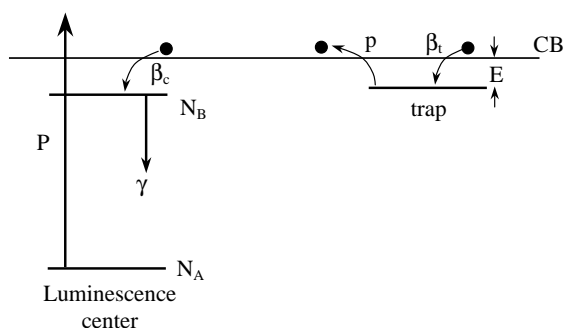


Fig. 1. Energy levels and electron transitions of a luminescent phosphor containing traps. P represents the irradiation process, whereby the luminescence centers are initially ionized, leading to the creation of populated traps, photo-ionized centers, and excited luminescence centers. The rate equations, Eqs. (2), describe the adjustments that take place after irradiation. The other terms in the figure are explained in the text.

act as the traps. Photoionization converts some of the Eu^{2+} ions to Eu^{3+} ions. We term these Eu^{3+} ions the *photo-ionized centers*. Electrons thermally released to the CB from the trap can recombine with the Eu^{3+} ions, releasing a photon characteristic of Eu^{2+} as described by the process [4]



In our generic model above, N is the density of traps, and n is the density of filled traps, n_c is the density of electrons in the CB. Charge neutrality requires that $N^+ = n + n_c$. Additionally, $N_A + N_B + N^+$ is the density of luminescence centers and is a constant. p , β_t , and β_c are the relevant transition probabilities, respectively, for a trapped electron to be thermally released to the CB, for a CB electron to become trapped at a trap center, and for a CB electron to recombine with an ionized luminescence center. p is of the form $se^{-E/kT}$, where E is the depth of the trap. s is termed the frequency factor. γ is the decay rate of centers in level B.

The processes at work after irradiation are described by a set of rate equations:

$$\frac{dN_A}{dt} = N_B\gamma, \quad (2.1)$$

$$\frac{dN_B}{dt} = n_c\beta_cN^+ - N_B\gamma, \quad (2.2)$$

$$\frac{dn}{dt} = -nse^{-E/kT} + \beta_t(N - n)n_c, \quad (2.3)$$

$$\frac{dn_c}{dt} = nse^{-E/kT} - n_c(\beta_t(N - n) + \beta_c N^+), \quad (2.4)$$

along with the equation $N_A + N_B + N^+ = \text{const.}$ (see above). The experimentally observed TL intensity is proportional to $N_B\gamma$.

These rate equations are analogous to the set describing the case of a recombination center (at which CB electrons recombine with holes in the valence band (VB)) and a trap, such as that discussed by McKeever [1]. To develop this analogy, we note that, in the case of the recombination center, the electron–hole recombination rate is $\beta_c n_c n_h$ [5], where n_h is the density of holes in the VB. In the case of the luminescence center described here, the CB electrons recombine with the ionized centers at a rate $\beta_c n_c N^+$. N^+ in the luminescence center model is the analog of n_h in the recombination center model. Because of charge neutrality, we have $n_h \cong n$ and $N^+ \cong n$, since it is expected that $n_c \ll n$.

As pointed out by McKeever [1], in order to obtain analytical solutions of the rate equations for the case of the recombination center and trap, two assumptions need to be made: (1) $n_c \ll n$, and (2) $|dn_c/dt| \ll |dn/dt|$. With these assumptions one obtains the equation [6]

$$\frac{dn}{dt} = \frac{-pn^2\beta_c}{\beta_c n + \beta_t(N - n)} = \frac{-pn^2}{n + R(N - n)}, \quad (3)$$

where $R = \beta_t/\beta_c$ and $p = se^{-E/kT}$.

If the probability of trapping is negligible compared with the probability of recombination, i.e. $\beta_c n \gg \beta_t(N - n)$, then the equation reduces to

$$\frac{dn}{dt} = -pn = -nse^{-E/kT}. \quad (4)$$

Processes based on Eq. (4) are said to follow *first order kinetics*. If the temperature of the material is raised from a low value T_0 at a linear heating rate, q , the shape of the TL glow curve, derived from this equation, is [7]

$$I(T) = n_0 s e^{-E/kT} \exp[-(s/q) \int_{T_0}^T e^{-E/kT} dT], \quad (5)$$

where n_0 is the density of trapped electrons at the initial temperature T_0 . If the retrapping process dominates, i.e. $\beta_c n \ll \beta_t(N - n)$, and if it is assumed that $N \gg n$, the rate equations yield the equation [8]

$$\frac{dn}{dt} = -n^2 \frac{s}{RN} e^{-E/kT}. \quad (6)$$

Processes based on $dn/dt \propto -n^2 e^{-E/kT}$, such as Eq. (6), are said to follow *second order kinetics*. The shape of the TL glow curve generated by Eq. (6) is given by Garlick and Gibson [9]

$$I(T) = n_0^2 \frac{s}{RN} e^{-E/kT} \left(1 + \frac{sn_0}{RNq} \int_{T_0}^T e^{-E/kT} dT \right)^{-2}. \quad (7)$$

The appearance before the integral of the initial filling factor $f = n_0/N$ (i.e. the fraction of traps initially filled with electrons) means that the shape of the TL glow curve for second order kinetics depends in part on the level of irradiation of the material before the measurement of the TL glow curve.

Along with the starting equations (4) and (6), which yield first and second order kinetics, respectively, a *general order* equation has been proposed [1,10]:

$$\frac{dn}{dt} = -n^b s' e^{-E/kT} \quad (8)$$

which yields a general order expression for the TL glow curve (valid for $b \neq 1$)

$$I(T) = n_0^b s' e^{-E/kT} \times \left(1 + (b-1)n_0^{b-1} \frac{s'}{q} \int_{T_0}^T e^{-E/kT} dT \right)^{-b/(b-1)}, \quad (9)$$

where b is the order of the kinetics.

Eq. (8) is not based on any physical model. Further, the factor, s' , has the units $(\text{cm})^{3(b-1)} \text{s}^{-1}$. Defining a new frequency factor $s'' = s' n_0^{b-1}$, Eq. (9) can be written as [11]

$$I(T) = n_0 s'' e^{-E/kT} \times \left(1 + (b-1) \frac{s''}{q} \int_{T_0}^T e^{-E/kT} dT \right)^{-b/(b-1)} \quad (10)$$

s'' now has the units s^{-1} , but, except for the cases of $b=1$ and 2, it is not related to any

particular physical quantity, in contrast to the frequency factors s which appear in the first and second order kinetics expressions.

It is useful to compare the general order expression for $I(T)$ (Eq. (10)) for the case of $b = 2$, with the second-order expression, Eq. (7). We see that when $b = 2$, the s'' factor in the general order expression is equal to $sn_0/(NR)$, where s is the frequency factor for the thermal release of electrons from traps, as shown in Fig. 1 and as used in Eq. (4).

Returning now to the model we are adopting for the luminescence center, we note that the movement of the electrons through the CB is the mechanism by which electrons, released from the traps, are either captured by the ionized luminescence centers or captured again by the trap (retrapping). Since the electrons spend very little time in the CB, we may be allowed to dispense with the time spent in this intermediate step, and look upon the process of electron release and capture as a process involving only the traps and the ionized luminescence centers. In that case, the rate equations become

$$\begin{aligned} \frac{dn}{dt} &= -\frac{pn\beta_c N^+}{\beta_c N^+ + \beta_t(N-n)} \\ &= -\frac{pn^2\beta_c}{\beta_c n + \beta_t(N-n)} \\ &= -\frac{pn^2}{n + R(N-n)}, \end{aligned} \quad (11.1)$$

where in obtaining the last two expressions, we have assumed that $n_c \ll n$, and hence that we can write $n = N^+$. Similarly

$$\frac{dN_B}{dt} = \frac{pn^2}{n + R(N-n)} - N_B\gamma. \quad (11.2)$$

We note that Eq. (11.1) above is exactly the same as that obtained from the rate equation analysis for the recombination center [8].

We observe that when $R = 1$, Eq. (11.1) becomes $dn/dt = -pn^2/N$, and the thermoluminescence process follows second-order kinetics for all values of the initial filling factor, $f = n_0/N$.

3. Generation of simulated TL glow curves

The “TL glow curves” in this study, $I_{TL}(T) \sim N_B$, were generated as numerical solutions to Eqs. (11) with the aid of the Maple 7 package using the Fehlberg fourth–fifth order Runge–Kutta method. In principle, there was no need to dispense with the free electron lifetime and to deal with Eqs. (11); exact solutions to Eqs. (2) can be obtained in the same way. However, solving Eqs. (11) is a considerably faster process, so that it is very tempting to deal with Eqs. (11) instead of Eqs. (2) — unless this simplification causes the results to deviate noticeably from the correct solutions. For selected sets of input parameters and initial conditions, we performed a comparison of the glow curves generated by the two methods. The results were similar to those obtained by Kelly et al. [12]: the free electron lifetime causes a certain delay between thermal ionization of traps and luminescence and thus makes the falling edges of the glow peaks longer. This effect becomes noticeable only when the lifetime of the free electrons is larger than, or comparable with, the temporal resolution of the TL experiment (typically 1 s).

For a particular system of interest, it is easy to find out whether Eqs. (11) can be used, or whether Eqs. (2) should be solved instead. The free electron lifetime can be estimated as $(v\sigma N)^{-1}$, where v is thermal velocity, σ is the electron capture cross-section, and N is the concentration of traps. Typical values of the electron capture cross-sections can be taken from the text by Bube [13]: 10^{-12} , 10^{-15} , and 10^{-19} cm² for Coulomb attraction, neutral, and Coulomb repulsion centers, respectively. The thermal velocity can be estimated as $\sqrt{2kT/m}$ (m is electron mass). Taking the room temperature value of v to be 10^7 cm s⁻¹, we find that even with the smallest known electron capture cross-section, 10^{-19} cm², it takes only a trap density of 10^{12} cm⁻³ to decrease the free electron lifetime to 1 s, a typical temporal resolution in TL experiments. In the cases of the neutral and Coulomb attraction traps, this marginal trap density value is 10^8 and 10^5 cm⁻³, respectively. It appears then that the use of Eqs. (11) is problematic only in the case of ultra-pure materials. In our systems of interest—doped luminescent

phosphors with a trap density of at least 10^{20} cm^{-3} , we have many orders of magnitude in reserve.

The simulated glow curves were fitted to Eq. (10), allowing values of b from unity upwards. The selection of starting parameters was not a significant issue; the fitting was just a matter of time, a smooth process with no effect of “local minima” noticed. As a criterion of fit quality, we used an averaged square deviation of the fit from the simulated glow curve. This is labelled “ Q ” in the tables.

4. Analysis of simulated TL glow curves

We consider three different arrangements of luminescence centers and traps. We generate simulated TL glow curves for each arrangement, using a range of trap parameters values. These glow curves are analyzed by the same method as are used to analyze experimentally measured TL glow curves—by fitting them to the general order intensity formula (Eq. (10))—and the parameter values determined by this fitting procedure are compared with the values used in generating the glow curves. We comment on the quality of the fit and on the accuracy of the parameter values.

4.1. Arrangement 1: luminescence centers with a single trap type

Fig. 2 shows a set of simulated glow curves for the following parameters: $E = 0.5 \text{ eV}$, $s = 10^{11} \text{ s}^{-1}$, initial filling $f = 0.1$, $q = 1 \text{ K s}^{-1}$, and for the range of values of $R (= \beta_t/\beta_c)$ as indicated. For each curve, a best fit was found to the general order expression for $I(T)$, and the parameter values derived from the fit, are listed in Table 1, along with the quality of the fit (Q).

Curve 2.1 was generated for $\beta_t = 0$, for which value Eq. (11.1) becomes $dn/dt = -pn$, and a first-order kinetics process is expected. We note that the shape of the glow curve, with its steeper fall off on the high temperature side, is characteristic of first-order kinetics [1]. This is confirmed by the fitting procedure, which yields $b = 1$ and the correct values of E and s to high accuracy. In the matter of

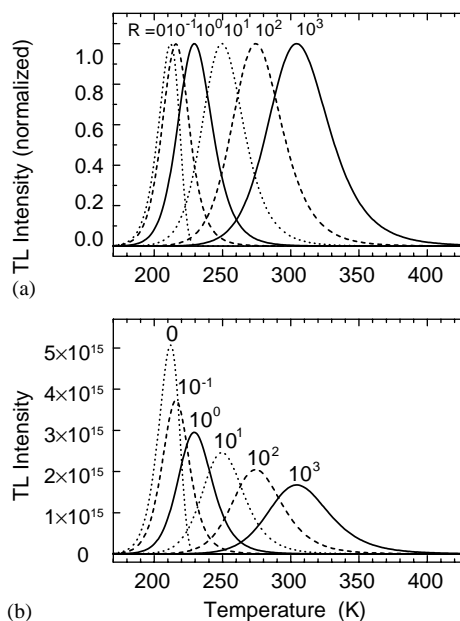


Fig. 2. Set of simulated glow curves for the case of a single trap type. The curves are generated for the values of $R = \beta_t/\beta_c$ indicated above the curve peaks. Other parameters: $E = 0.5 \text{ eV}$, $s = 10^{11} \text{ s}^{-1}$, initial filling $f = 0.1$, $q = 1 \text{ K s}^{-1}$. All curves on Fig. 2a are normalized to unity at maximum intensity. The curves in Fig. 2b show the correct relative areas.

the fitting of curve 2.1, we can show that, whereas the general order expression, Eq. (10), is not valid for $b = 1$, Eq. (9) converts to the first-order expression, Eq. (5), in the limit, as b approaches unity. Thus the s'' factor for $b = 1$ is identical with the frequency factor for the thermal release of electrons from the trap: $p = se^{-E/kT}$.

As we observed in Section 2, when $R = 1$ (curve 2.3), the process will be accurately described by second-order kinetics. As Table 1 shows, one obtains an excellent fit, yielding the expected value of b and giving E to high accuracy. Since for $b = 2$, we have $s'' = sn_0/(NR)$, which is $s 10^{-1}$ in this case, and the fitting yields the value of s to high accuracy. For curves 2.4–2.6, for which $R > 1$ and which represent situations where retrapping is dominant, we do not obtain a similar quality of fit, and the values of b , E , and s are not as accurate. To understand this, we note that, in the case where $\beta_t > \beta_c$ ($R > 1$), Eq. (11.1) does not conform to the general order rate equation (Eq. (8)). As a result,

Table 1
Analysis of the simulated glow curves of Fig. 2, generated for different values of R , for the case of a single trap type

Curve	Varied parameter $R = \beta_t/\beta_c$	Values derived from fitting				
		b	E (eV)	s'' (s ⁻¹)	s (s ⁻¹) ^a	Q
2.1	0	1.0000	0.5000	1.0000×10^{11}	1.0000×10^{11}	5×10^{-14}
2.2	10^{-1}	1.68	0.50	6×10^{10}	^b	2×10^{-5}
2.3	1	1.99980	0.500	9.98×10^9	9.98×10^{10}	5×10^{-11}
2.4	10	2.057	0.500	1.1×10^9	1.1×10^{11}	1×10^{-6}
2.5	10^2	2.05	0.498	1.0×10^8	1.0×10^{11}	1×10^{-6}
2.6	10^3	2.04	0.496	9.2×10^6	9.2×10^{10}	7×10^{-7}

Unvaried input parameters values: $E = 0.5$ eV, $s = 10^{11}$ s⁻¹, $q = 1$ K s⁻¹, $\gamma = 100$ s⁻¹, $f = n_0/N = 0.1$. The uncertainty in the values derived from the fitting are less than the least significant figure in each case.

^aFor values of b very close to 2, we use $s'' = sn_0/(NR)$.

^bAs explained in the text, the relationship between s'' and s is only known accurately for $b = 1$ and $b = 2$. For values of b very close to $b = 1$ or 2, we may expect these relationship to hold approximately. For curve 2.2 above, we are unable to infer a value of s from the measured value of s'' .

the glow curve will not be accurately described by the general order formula, Eq. (10), with the consequential inherent inaccuracy in the fitting of the glow curve to Eq. (10) and in the values derived for b , E , and s . Nevertheless, the closeness of b to 2 shows that the second-order process dominates, and the values obtained for E and s are close to the correct trap values.

A point to be stressed here is that the dominance of retrapping is not an exact criterion for a second-order process in which the TL glow curve fits Eq. (7); rather the criterion for a TL glow curve to fit Eq. (7) is that the rate equation governing the process should have the form $dn/dt \propto -pn^2$.

We note that curve 2.2, for which $R = 10^{-1}$, yields a b values between 1 and 2, and is fitted with much less accuracy by the general order equation. The reason is again to be found in Eq. (11.1), where it is seen that, for these values of R , Eq. (11.1) does not conform to a general order rate equation (Eq. (8)). We do not have a physical interpretation for s'' in this intermediate regime where b values are between 1 and 2, but the value of s'' is within a factor of 2 of the input s value.

Fig. 3 shows a set of simulated glow curves where the initial filling factor $f = n_0/N$ is varied while keeping the other input parameter values fixed at $E = 0.5$ eV, $s = 10^{11}$ s⁻¹, $q = 1$ K s⁻¹, $R = 1$ (i.e. $\beta_t = \beta_c$). Table 2 gives the parameter values derived from the best fits to the general order

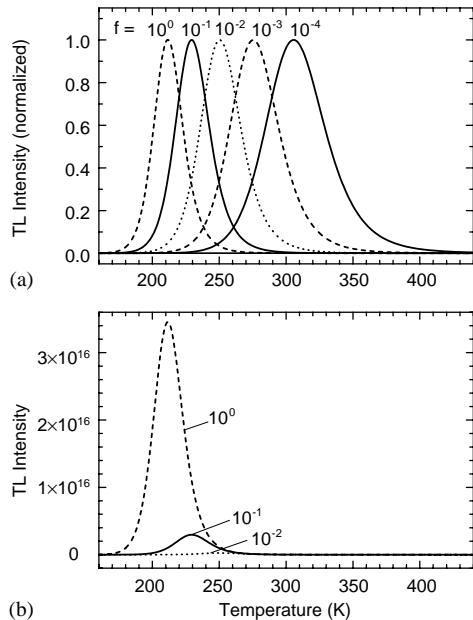


Fig. 3. Set of simulated glow curves for the case of a single trap type. The curves are generated for the values of the initial filling factor $f = n_0/N$ indicated above the curve peaks. Other parameters: $E = 0.5$ eV, $s = 10^{11}$ s⁻¹, $q = 1$ K s⁻¹, $R = \beta_t/\beta_c = 1$. All curves on Fig. 3a are normalized to unity at maximum intensity. The curves in Fig. 3b show the correct relative areas.

equation. As can be seen, all curves conform to a second-order process, yielding values of E and s to high accuracy. This is expected, since, as we have seen, for $R = 1$ Eq. (11.1) conforms exactly to a

Table 2

Analysis of the simulated glow curves of Fig. 3, generated for different values of the filling factor f , when a single trap type is present

Curve	Varied parameter	Values derived from fitting				
	$f = n_0/N$	b	E (eV)	s'' (s^{-1})	s (s^{-1}) ^a	Q
3.1	10^{-4}	2.00031	0.5000	1.0000×10^7	1.0000×10^{11}	3×10^{-12}
3.2	10^{-3}	2.00016	0.5000	1.0000×10^8	1.0000×10^{11}	6×10^{-13}
3.3	10^{-2}	2.00010	0.5000	1.0000×10^9	1.0000×10^{11}	2×10^{-13}
3.4	10^{-1}	1.99980	0.5000	9.98×10^9	9.98×10^{10}	5×10^{-11}
3.5	1	1.99978	0.5000	9.98×10^{10}	9.98×10^{10}	4×10^{-11}

Unvaried input parameters: $E = 0.5$ eV, $s = 10^{11}$ s^{-1} , $q = 1$ K s^{-1} , $R = 1$. The uncertainty in the values derived from the fitting process are less than the least significant figure in each case.

^aThe value of s is obtained from $s'' = sn_0/(NR)$.

second-order rate equation, and a good fit to the $b = 2$ glow curve formula is expected.

4.2. Arrangement 2: pre-ionized and photo-ionized luminescence centers with a single trap type

In this arrangement, we allow for the presence of pre-ionized luminescence centers before the excitation process begins. (In our illustrative example, this is the arrangement where Eu^{2+} and Eu^{3+} centers co-exist before excitation. We refer to these Eu^{3+} ions as the pre-ionized centers. During the excitation process, some of the Eu^{2+} ions will be photo-ionized to Eu^{3+} centers.) M is the density of pre-ionized centers, and N^+ is the density of photo-ionized centers. Charge compensation for these M pre-ionized centers may contribute to the existence of traps.

For this arrangement, the rate equations, Eq. (11), are modified by replacing N^+ by $N^+ + M$, and Eq. (11.1) becomes

$$\begin{aligned} \frac{dn}{dt} &= -\frac{pn\beta_c(N^+ + M)}{\beta_c(N^+ + M) + \beta_t(N - n)} \\ &= -\frac{pn(n + M)}{(n + M) + R(N - n)} \end{aligned} \quad (12)$$

where $R = \beta_t/\beta_c$. There is a similarity between the inclusion of M pre-ionized centers in our model and the inclusion of M thermally disconnected traps in the recombination model, as discussed by McKeever [1] and other workers [14]. In our case,

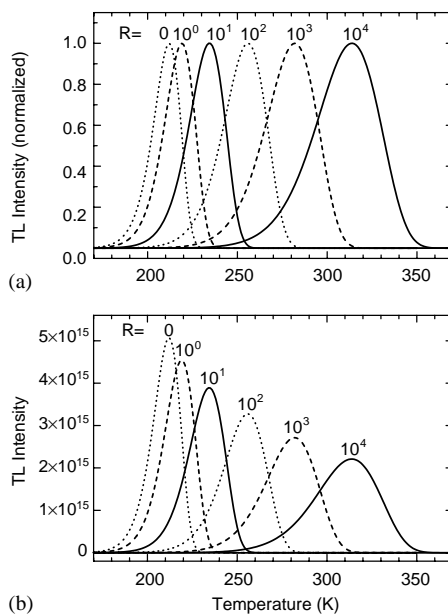


Fig. 4. Set of simulated glow curves for the case where pre-ionized centers are present. The values of $R = \beta_t/\beta_c$ are indicated above the curve peaks. Other parameters: $E = 0.5$ eV, $s = 10^{11}$ s^{-1} , $q = 1$ K s^{-1} , $\gamma = 100$ s^{-1} , $N = 10^{20}$ cm^{-3} , $M = 5 \times 10^{19}$ cm^{-3} (the density of pre-ionized centers). In Fig. 4a, all curves are normalized to unity at maximum intensity. The curves in Fig. 4b show the correct relative areas.

however, the M traps are optically active ions, and when they trap electrons, they participate in the luminescence process.

Fig. 4 shows a set of simulated glow curves for the case where pre-ionized centers are

present. These curves are derived from Eq. (12). The parameters are $E = 0.5$ eV, $s = 10^{11}$ s⁻¹, $q = 1$ K s⁻¹, $\gamma = 100$ s⁻¹, $N = 10^{20}$ cm⁻³, M (the density of pre-ionized centers) = $5 \cdot 10^{19}$ cm⁻³, and the value of R is varied, as indicated. For $R = 0$, Eq. (12) becomes $dn/dt = -pn$, and the glow curve is expected to be accurately described by first-order kinetics. This is confirmed by the fitting procedure, which yields $b = 1$ and the correct values of E and s to high accuracy (Table 3). For other values of R , we can see that Eq. (12) does not conform to the general order rate equation, hence attempts to describe the resultant glow curves by the general order formula, Eq. (10), cannot be expected to have high accuracy. This is confirmed by the much poorer quality of fit seen in Table 3, compared with the $R = 0$ case. For small non-zero values of R , Eq. (12) is approximately expressed as $dn/dt = -pn$, and the parameters derived from the fitting process are close to the input values. Analysis of Eq. (12) for larger values of R indicates that the deviation from a pure general order rate equation increases with increasing R , that the process is still close to first order, and that the value of s'' should decrease as $1/R$. These trends are seen in the parameter values obtained from the fitting procedure (Table 3).

Fig. 5 shows a set of simulated glow curves for the case where pre-ionized centers are present, where the initial filling $f = n_0/N$ is varied, while the values of the other parameters are held

constant at $E = 0.5$ eV, $q = 1$ K s⁻¹, $s = 10^{11}$ s⁻¹, $\gamma = 100$ s⁻¹, $N = 10^{20}$ cm⁻³, $M = 5 \times 10^{19}$ cm⁻³, $R = 1$. The values of the parameters derived from the fitting procedure are given in Table 4.

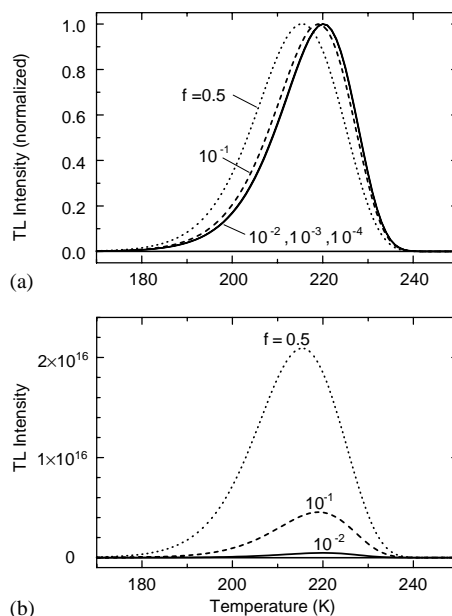


Fig. 5. Set of simulated glow curves for the case where pre-ionized centers are present. The values of the initial filling $f = n_0/N$ are indicated. Other parameters: $E = 0.5$ eV, $s = 10^{11}$ s⁻¹, $q = 1$ K s⁻¹, $\gamma = 100$ s⁻¹, $N = 10^{20}$ cm⁻³, $M = 5 \times 10^{19}$ cm⁻³ (the density of pre-ionized centers), $R = \beta_i/\beta_c = 1$. All curves in Fig. 5a are normalized to unity at maximum intensity. The curves in Fig. 5b show the correct relative areas.

Table 3

Analysis of the simulated glow curves of Fig. 4, for the case where pre-ionized luminescent centers and a single trap type are present

Curve	Varied parameter	Values derived from fitting				
	$R = \beta_i/\beta_c$	b	E (eV)	s'' (s ⁻¹)	s (s ⁻¹) ^a	Q
4.1	0	1.00001	0.5000	1.0013×10^{11}	1.0013×10^{11}	6×10^{-14}
4.2	1	1.03	0.485	1.6×10^{10}		2×10^{-6}
4.3	10	1.05	0.477	1.8×10^9		5×10^{-6}
4.4	10^2	1.05	0.476	2.0×10^8		7×10^{-6}
4.5	10^3	1.05	0.476	2.2×10^7		8×10^{-6}
4.6	10^4	1.05	0.476	2.4×10^6		9×10^{-6}

The glow curves are drawn for different values of R . The fixed parameter values are: $E = 0.5$ eV, $s = 10^{11}$ s⁻¹, $q = 1$ K s⁻¹, $\gamma = 100$ s⁻¹, $f = n_0/N = 0.1$, $N = 10^{20}$ cm⁻³, $M = 5 \times 10^{19}$ cm⁻³. The uncertainty in the values derived from the fitting are less than the least significant figure in each case.

^aWhen $b = 1$, $s'' = s$. For values of b very close to 1 we may expect $s'' \cong s$, but we observe that for $b > 1.01$ the values of s'' deviate markedly from the input s value and we are unable to infer a relationship between s'' and s .

Table 4

Analysis of the simulated glow curves of Fig. 5, for the case where pre-ionized luminescent centers and a single trap type are present

Curve	Varied parameter	Values derived from fitting				
	$f = n_0/N$	b	E (eV)	s'' (s^{-1})	s (s^{-1}) ^a	Q
5.1	10^{-4}	1.00004	0.5000	3.3343×10^{10}	1.000×10^{11}	5×10^{-12}
5.2	10^{-3}	1.0003	0.4999	3.308×10^{10}		3×10^{-10}
5.3	10^{-2}	1.003	0.4982	3.06×10^{10}		3×10^{-8}
5.4	10^{-1}	1.03	0.485	1.6×10^{10}		3×10^{-6}
5.5	0.5	1.2	0.48	1.9×10^9		5×10^{-5}

The glow curves are drawn for different values of the initial filling factor, f . The fixed parameter values are: $E = 0.5$ eV, $s = 10^{11}$ s^{-1} , $q = 1$ K s^{-1} , $R = 1$, $\gamma = 100$ s^{-1} , $N = 10^{20}$ cm^{-3} , $M = 5 \times 10^{19}$ cm^{-3} . The uncertainty in the values derived from the fitting are less than the least significant figure in each case.

^a As explained in the text, for very small f values we can derive a relationship between s'' and s , but as the filling factor increases, the process proceeds by a mixture of first- and second-order statistics, which prevents us from inferring a value of s from the measures s'' value.

When $R = 1$, Eq. (12) becomes

$$\begin{aligned} dn/dt &= -pn(n + M)/(M + N) \\ &= -pn^2/(M + N) - pnM/(M + N) \end{aligned} \quad (13)$$

indicating that the process proceeds by a mixture of first and second order kinetics. In general, then, the process described by Eq. (13) cannot be accurately described by the general order rate equation (Eq. (9)), so attempts to describe the resultant glow curve by the general order formula (Eq. (11)) should not be expected to have high accuracy. The value of b derived from a fitting procedure will fall between 1 and 2. If the initial filling is such that $n_0 \ll N$, M , then the second-order process above can be neglected, Eq. (13) becomes $dn/dt = -pnM/(M + N)$, and the process proceeds by first-order kinetics, with an effective frequency factor: $sM/(M + N) = s/3$ for the parameter values chosen here. This is in agreement with the parameter values in Table 4 for $f = 10^{-4}$, and the quality of the fit is high. As f increases, the deviation of Eq. (13) from an exact general order rate equation increases, and the quality of the fit decreases. When the initial filling is large ($n_0 \approx N$, M), the contribution from the second-order process is significant. This is reflected in the results of the fitting procedure, where a value of b of 1.23 is obtained for $f = 0.5$.

In regard to Eq. (13), which indicates that under certain conditions the process proceeds by a

mixture of first- and second-order kinetics, there is an interesting paper by Chen et al. [15] that argues that a mixed order equation may also be used as an empirical approximation to the set of differential equations governing the TL process. These authors point out that the mixed order approach has a number of advantages compared with the more commonly employed general order equation (Eq. (8)).

4.3. Arrangement 3: luminescence centers with two inequivalent traps

Experimentally-observed TL spectra are often characterized by a number of peaks indicating that more than one type of trap is involved. In this arrangement, two inequivalent trap types are considered, and the electrons from the photo-ionized luminescence centers are assumed to be able to enter either trap. This is the situation expected if the trapping and retrapping occurs through the CB. When the temperature is raised so that trapped electrons are thermally released from the shallower trap, these electrons may go either to the luminescence center or to the deeper trap. The reduction in the flow of the thermally released electrons from the shallower trap to the luminescence center can result in a significant change in the shape and intensity of the glow curve due to a shallower trap compared with that observed in the absence of a deeper trap. Since the separate peaks

in experimentally-observed TL spectra are usually analyzed on the implicit assumption that the different traps, in their interaction with the luminescence center, act independently of each other, such an analysis can give misleading values of the trap parameters. The importance of taking into account the transfer of electrons between traps has been stressed by Chen and McKeever [2] and has been pointed out again by Sakurai [16] in a more recent study.

For the case of two traps, Eqs. (11.1) and (11.2) are modified to read

$$\begin{aligned} \frac{dn_1}{dt} &= \frac{-p_1 n_1 (\beta_c N^+ + \beta_{t2} (N_2 - n_2))}{\beta_c N^+ + \beta_{t1} (N_1 - n_1) + \beta_{t2} (N_2 - n_2)} \\ &\quad + \frac{p_2 n_2 (\beta_{t1} (N_1 - n_1))}{\beta_c N^+ + \beta_{t1} (N_1 - n_1) + \beta_{t2} (N_2 - n_2)}, \\ \frac{dn_2}{dt} &= \frac{-p_2 n_2 (\beta_c N^+ + \beta_{t1} (N_1 - n_1))}{\beta_c N^+ + \beta_{t1} (N_1 - n_1) + \beta_{t2} (N_2 - n_2)} \\ &\quad + \frac{p_1 n_1 (\beta_{t2} (N_2 - n_2))}{\beta_c N^+ + \beta_{t1} (N_1 - n_1) + \beta_{t2} (N_2 - n_2)}, \\ \frac{dN_B}{dt} &= \frac{(p_1 n_1 + p_2 n_2) \beta_c N^+}{\beta_c N^+ + \beta_{t1} (N_1 - n_1) + \beta_{t2} (N_2 - n_2)} - N_B \gamma, \end{aligned} \quad (14)$$

where $N^+ = n_1 + n_2$.

Simulated TL glow curves were generated for various values of the parameters of the traps. The peaks were analyzed by the usual fitting procedure applied separately to each peak, as is normally done for experimental TL spectra.

Fig. 6 shows the simulated glow curves generated for the case of two traps with parameters $E_1 = 0.35$ eV, $f_1 = 0.05$, $s_1 = 10^{12}$ s⁻¹, $\beta_{t1} = \beta_c$, $E_2 = 0.5$ eV, $f_2 = 0.05$, $s_2 = 10^{12}$ s⁻¹, $\beta_{t2} = \beta_c$; $f_c = 0.1$ and $\gamma = 100$ s⁻¹. The concentrations of the luminescence centers and of each of the traps are equal. f_1 and f_2 are the initial filling factors for the two traps. f_c is the initial fraction of luminescence centers that are ionized, and in this example, $f_c = f_1 + f_2$. There are no pre-ionized luminescence centers. The two separate broken curves in Fig. 6 are the predicted glow curves when the traps act independently. The areas under the curves are equal, as expected. Because $\beta_{t1} = \beta_{t2} = \beta_c$, the processes are expected to follow second order kinetics. The light full curve is the predicted TL

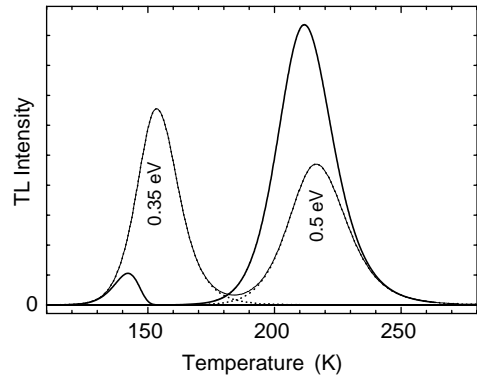


Fig. 6. Simulated glow curves for the case where two traps are present. Trap parameters: $E_1 = 0.35$ eV, $f_1 = 0.05$, $s_1 = 10^{12}$ s⁻¹, $\beta_{t1} = \beta_c$ and $E_2 = 0.5$ eV, $f_2 = 0.05$, $s_2 = 10^{12}$ s⁻¹, $\beta_{t2} = \beta_c$. The concentrations of the luminescence centers and of each of the traps are equal. The two dotted curves are the glow curves when the traps act independently, and the light full curve is their sum. The heavy full curve is the TL spectrum generated for the case where there is electron exchange between traps.

spectrum when both traps are active in the material, but are acting independently of each other. The heavy full curve is the predicted TL spectrum based on Eq. (14), where the transfer of electrons between traps can occur. We observe that the peak due to the shallower trap is greatly reduced in intensity, and the shape is characteristic of first-order kinetics. Its maximum has shifted to lower temperature. The peak due to the deeper trap has increased in intensity and its maximum has also shifted to lower temperature.

A series of such simulated TL spectra were generated for the same two traps, with different values of the initial filling factors; $f_1 = f_2$ in each case. The results of the fitting process, where the glow curves due to each of the traps were fitted to the general order formula, Eq. (10), are shown in Table 5 for three sets of values for the initial filling factors (f_1, f_2) : 0.005, 0.05, 0.5. In each case $f_c = f_1 + f_2$.

The area under the lower temperature TL curve relative to that of the higher temperature curve is strongly dependent on the initial filling factors, f_1 and f_2 . If $f_1 = f_2 = 0.5$, the ratio is approximately 0.5. If $f_1 = f_2 = 0.05$, as in the case illustrated in Fig. 6, the ratio falls by an order of magnitude,

Table 5

Analysis of simulated glow curves generated for the case where two inequivalent interacting trap type are present

Trap	Input $f_1 (=f_2)$	Values derived from fitting		
		b	E (eV)	s'' (s^{-1})
1	0.005	1.0007(4)	0.34969(3)	$4.88(1) \times 10^{11}$
2	0.005	2.00024	0.500016(2)	9.94×10^9
1	0.05	1.008(1)	0.3469(2)	$3.99(5) \times 10^{11}$
2	0.05	1.9999	0.49999(3)	$9.51(2) \times 10^{10}$
1	0.5	1.10(1)	0.333(2)	$1.6(2) \times 10^{11}$
2	0.5	2.008(4)	0.502(2)	$7.4(9) \times 10^{11}$

Three sets of values for the initial filling factors, f_1 and f_2 are used, as shown. Other input parameters values are: $E_1 = 0.35$ eV, $E_2 = 0.5$ eV, $s_1 = s_2 = 10^{12} s^{-1}$, $\beta_{i1} = \beta_{i2} = \beta_c$, $\gamma = 100 s^{-1}$. The uncertainty in the values derived from the fitting are less than the least significant figure in each case.

while if $f_1 = f_2 = 0.005$, the ratio falls by yet another order of magnitude. This indicates that information about a possible transfer of electrons between traps may be gained by measuring TL spectra under significantly different initial pumping conditions.

We observe that, when the traps can share electrons, the glow curve derived from the shallower trap is characterized by $b \approx 1$, for all values of the initial filling factors. For these same parameter values, if the traps are acting independently, the curve is characterized by $b = 2$. It is not the intrinsic parameter values of the trap that lead to the $b \approx 1$ characterization, rather it is the result of the interaction with the second trap. This should be borne in mind in the analysis of experimentally observed multi-trap TL spectra.

If the second trap is much deeper than the first trap, then the glow curve due to the deeper trap, since it peaks at a much higher temperature, may not manifest itself over the temperature range of the experimentally observed spectrum. The spectrum may indicate only the low temperature glow curve. The form of the low temperature glow curve, nevertheless, is strongly affected by the second trap. In analyzing experimental TL spectra which exhibit a single TL glow curve characterized by $b = 1$, the possibility of an undetected high temperature trap should be kept in mind.

By modifying the rate equations suitably, one can take into account the existence of pre-ionized luminescence centers. In this case, the shape of the lower peak is again modified, giving $b \approx 1$, but the variation with filling factors in the relative sizes of the two peaks is much smaller.

For all the simulated curves generated so far in this study, despite the wide range of parameter values used, the fitting procedures always indicated values of b between 1 and 2. However, in experimentally measured TL spectra, curves with shapes characterized by values of b greater than 2 are often reported. We explore the possibility that such large b values can be obtained when two or more traps, very close in energy, exist in the material. The broken curves in Fig. 7 are the simulated glow curves generated for two traps, with energies $E_1 = 0.48$ eV and $E_2 = 0.50$ eV, acting separately. The light full curve is the TL spectrum when both traps act independently. The heavy full curve is the TL spectrum when electrons can be shared between the traps. This has the appearance of a single peak. If this curve is analyzed by the usual fitting procedure, assuming that it is due only to a single trap, it yields a value of $b = 2.33$. Clearly, a cluster of traps, all very close in energy, can create a TL spectrum having the shape of a single peak with a value of b significantly larger than 2.

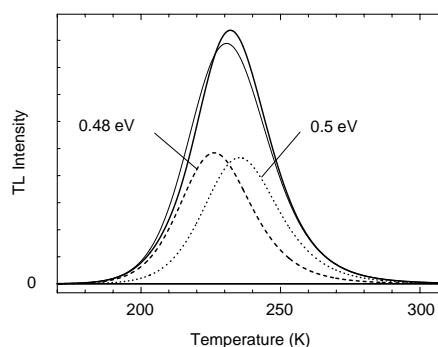


Fig. 7. Simulated glow curves for the case of two traps with similar trap depths. Trap parameters: $E_1 = 0.48$ eV, $E_2 = 0.5$ eV, $f_1 = f_2 = 0.05$, $s_1 = s_2 = 10^{11} s^{-1}$, $\beta_{i1} = \beta_{i2} = \beta_c$. The concentrations of the luminescence centers and of each of the traps are equal. The two broken curves are the glow curves when the traps act independently, and the light full curve is their sum. The heavy full curve is the TL spectrum generated for the case where there is electron exchange between traps.

5. Conclusion

The generation and analysis of TL spectra of luminescent materials carried out in this study show that the shape, intensity, and position of a glow curve can depend not only on the intrinsic parameters of the relevant trap but also on the presence of other traps, on the presence of pre-ionized luminescence centers, and on the level of excitation used to create the TL spectrum. The study has highlighted a number of factors that may assist in the interpretation and understanding of experimentally observed thermoluminescence spectra. These are summarized here.

- While the fitting process can provide values of E with reasonable accuracy, the values of s'' , derived from the process of fitting the experimental curve to Eq. (10), can differ by orders of magnitude from the true frequency factor of the trap (s).
- For a luminescence center with a single trap, without pre-ionized centers, the TL glow curve is likely to be characterized by $b \approx 2$. A value of $b \approx 1$ only occurs when $\beta_t \ll \beta_c$, that is, when retrapping is exceedingly weak. For such a center, $s'' = s$ when $b = 1$. When $b = 2$, $s'' = sn_0/(NR)$. Hence, to obtain an accurate estimate of s from the observed s'' value, one requires additional information on the initial filling $f = n_0/N$ and on $R = \beta_t/\beta_c$.
- If pre-ionized luminescence centers are present, the glow curve is likely to be characterized by $b \cong 1$. The value of s'' will depend on the initial filling.
- If the TL spectrum contains two or more glow curves, and if the lower temperature curves are weak and characterized by $b \cong 1$, this may indicate that the traps are interacting (i.e. sharing electrons). A strong variation with initial filling factor (i.e. excitation) of the relative area under the lower temperature curve is a characteristic of interacting traps.
- For experimental reasons, a glow curve due to a second much deeper trap may not manifest itself in an experimental TL spectrum. Such a trap will, nevertheless, affect the intensity and shape of the low temperature trap.
- Glow curves characterized by values of b greater than 2 may be caused by the presence of two or more traps with similar trap energies. Fitting such curves to the single trap model using Eq. (10), gives values of E close to the actual mean value for the traps, but the s'' value can be very different from the s values of the individual traps.

Acknowledgements

This work was supported by the National Science Foundation under grant number DMR 99–86693. The authors thank Prof. W. M. Dennis for helpful comments and suggestions. SB and GFI acknowledge the hospitality of the Department of Physics and Astronomy at the University of Georgia, Athens, Georgia, where the work was carried out.

References

- [1] S.W.S. McKeever, Thermoluminescence of Solids, Cambridge University Press, Cambridge, 1985.
- [2] R. Chen, S.W.S. McKeever, Theory of Thermoluminescence and Related Phenomena, World Scientific, Singapore, 1997.
- [3] C. Furetto, Pao-Shan Weng, Operational Thermoluminescence Dosimetry, World Scientific, Singapore, 1998.
- [4] I. Aguirre de Carcer, G. Lifante, F. Cusso, F. Jaque, T. Calderon, Appl. Phys. Lett. 58 (1991) 1825.
- [5] S.W.S. McKeever, Thermoluminescence of Solids, Cambridge University Press, Cambridge, 1985, Eq. (2.18), putting $\beta_c = A_r$.
- [6] S.W.S. McKeever, Thermoluminescence of Solids, Cambridge University Press, Cambridge, 1985, Eq. (3.4).
- [7] J.T. Randall, M.H.F. Wilkins, Proc. Roy. Soc. London 184 (1945) 366.
- [8] S.W.S. McKeever, Thermoluminescence of Solids, Cambridge University Press, Cambridge, 1985, Eq. (3.14).
- [9] G.F.J. Garlick, A.F. Gibson, Proc. Phys. Soc. 60 (1948) 574.
- [10] C.E. May, J.A. Partridge, J. Chem. Phys. 40 (1964) 1401.
- [11] S.W.S. McKeever, Thermoluminescence of Solids, Cambridge University Press, Cambridge, 1985, Eq. (3.16).
- [12] P.J. Kelly, M.J. Laubitz, P. Bräunlich, Phys. Rev. B 4 (1971) 1960.
- [13] R.H. Bube, Photoconductivity of Solids, Wiley, New York, 1960, pp. 60–62.
- [14] P.J. Kelly, P. Bräunlich, Phys. Rev. B 1 (1970) 1587.
- [15] R. Chen, N. Kristianpoller, Z. Davidson, R. Visocekas, J. Lumin. 23 (1981) 293.
- [16] T. Sakurai, J. Phys. D 34 (2001) L105.